Electronic Supplementary Material (ESI) for Physical Chemistry Chemical Physics.

Supplementary Information

Accelerated Acquisition of Wideline Solid-State NMR Spectra of Spin 3/2 Nuclei by Frequency-Stepped Indirect Detection Experiments

*Sujeewa N. S. Lamahewage[1,2], Benjamin A. Atterberry[1,2], Rick W. Dorn,[1,2], Eunbyeol Gi[1,2], Maxwell R. Kimball,[3] Janet Blümel[3] *, Javier Vela[1,2], Aaron J. Rossini[1,2] **

[1]*US Department of Energy, Ames National Laboratory, Ames, Iowa, USA, 50011*

[2]*Iowa State University, Department of Chemistry, Ames, IA, USA, 50011*

[3]*Texas A&M University, Department of Chemistry, College Station, Texas, USA, 77842*

AUTHOR INFORMATION

Corresponding Author

* e-mail: arossini@iastate.edu, phone: 515-294-8952.
* e-mail: bluemel@tamu.edu, phone: 979-845-7749.

Table of Contents

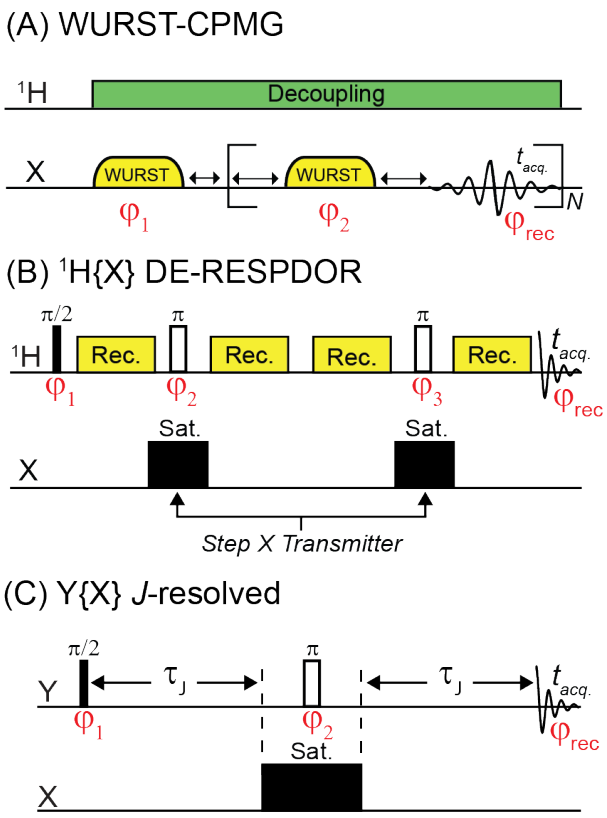

Figure S1. (A-C) Pulse sequence diagrams with phase labels for pulses and receiver. Phase cycles are given in Table S1.

Table S1. Phase cycles of the pulse sequences used in this paper.

Pulse Sequence	Phase Cycles
WURST-CPMG	φ_1 0 0 1 1 2 2 3 3 φ_2 1 3 2 0 3 1 0 2 φ_{rec} 0 0 1 1 2 2 3 3
1H{X} DE-RESPDOR	φ_1 0 2 φ_2 0 0 1 1 2 2 3 3 φ_3 {0}*8 {1}*8 {2}*8 {3}*8 φ_{rec} 0 2 2 0 0 2 2 0 2 0 0 2 2 0 0 2
Y{X} *J*-resolved	φ_1 0 0 2 2 φ_2 0 2 0 2 2 0 2 0 1 3 1 3 3 1 3 1 φ_{rec} {0 0 2 2}*2 {2 2 0 0}*2

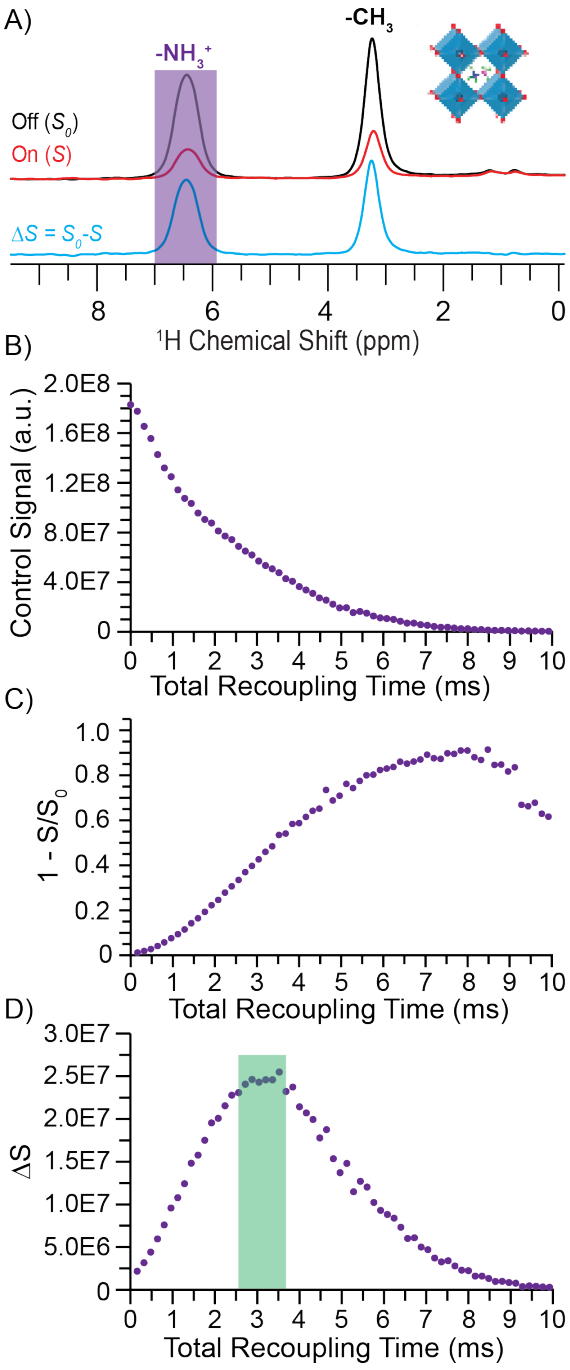

Figure S2. (A) 1D $^{1}H\{^{35}Cl\}$ DE-RESPDOR spectra recorded (red) with or (black) without a ^{35}Cl saturation pulse and 2.4 ms of $SR4_1^2$ dipolar recoupling for $MAPbCl_3$. A difference spectrum (cyan) is shown below. (B) The control signal (S_0), (C) Normalized dephasing ($\Delta S/S_0$), (D) Absolute dephasing (ΔS) as a function of total recoupling time in steps of 0.16 ms up to a total of 9.92 ms.

Discussion of Figure S2. Figure S2-A depicts $^{1}H\{^{35}Cl\}$ DE-RESPDOR spectra (red), with saturation pulses and spectra (black), without saturation pulses. With 16 scans, the control and dephasing

spectra have signal-to-noise ratios of 150 and 52, respectively. The difference spectrum (cyan) shown below has a signal-to-noise ratio of 73, allowing for the indirect detection of ^{35}Cl in $MAPbCl_3$. The spectra shown in Figure S2-A correspond to the 0 MHz ^{35}Cl offset. All spectra were collected at B_0 = 9.4 T using a ^{35}Cl saturation pulse length of four rotor cycles (80 µs) with an 80 kHz RF field and 3.84 ms of $SR4_1^2$ dipolar recoupling. The highlighted (purple) peak corresponding to ammonium was used to plot the graphs shown in Figure S2-B, C, and D. As shown in Figure S2-B, the control signal (S_0) is plotted as a function of total recoupling time in steps of 0.16 ms up to 9.92 ms. The graph in Figure S2-C shows the normalized dephasing [$(S_0\text{-}S)/S_0 = \Delta S/S_0$] as a function of total recoupling duration. The graph Figure S2-D plots the absolute dephasing [$(S_0\text{-}S) = \Delta S$)] as a function of total recoupling time. According to the plot (Figure S2-D), the optimal recoupling time range for the ^{1}H{^{35}Cl} DE-RESPDOR experiment is *ca.* 2.5 to 4 ms.

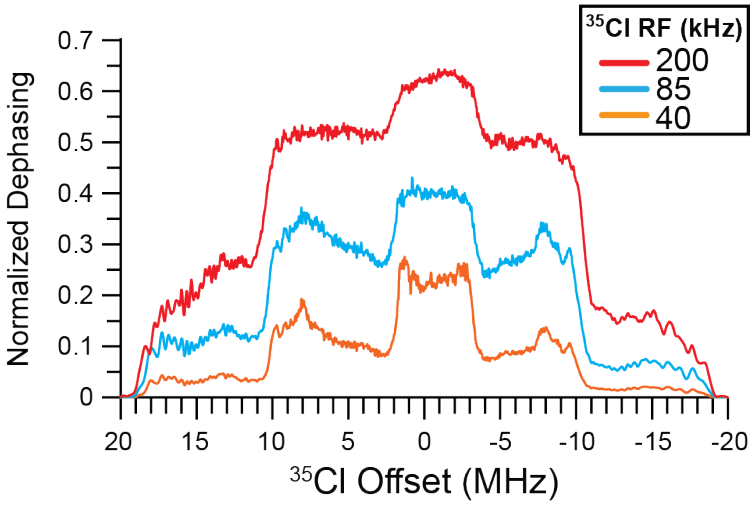

Figure S3. Simulated ^{1}H{^{35}Cl} DE-RESPDOR dephasing profiles for rectangular 40 µs saturation pulses. Simulations were performed with saturation pulse RF fields of 40 kHz, 85 kHz, and 200 kHz. Simulations used a ^{1}H-^{35}Cl spin system with a 2 kHz dipolar coupling constant, C_Q = 37 MHz and η_Q = 0.1.

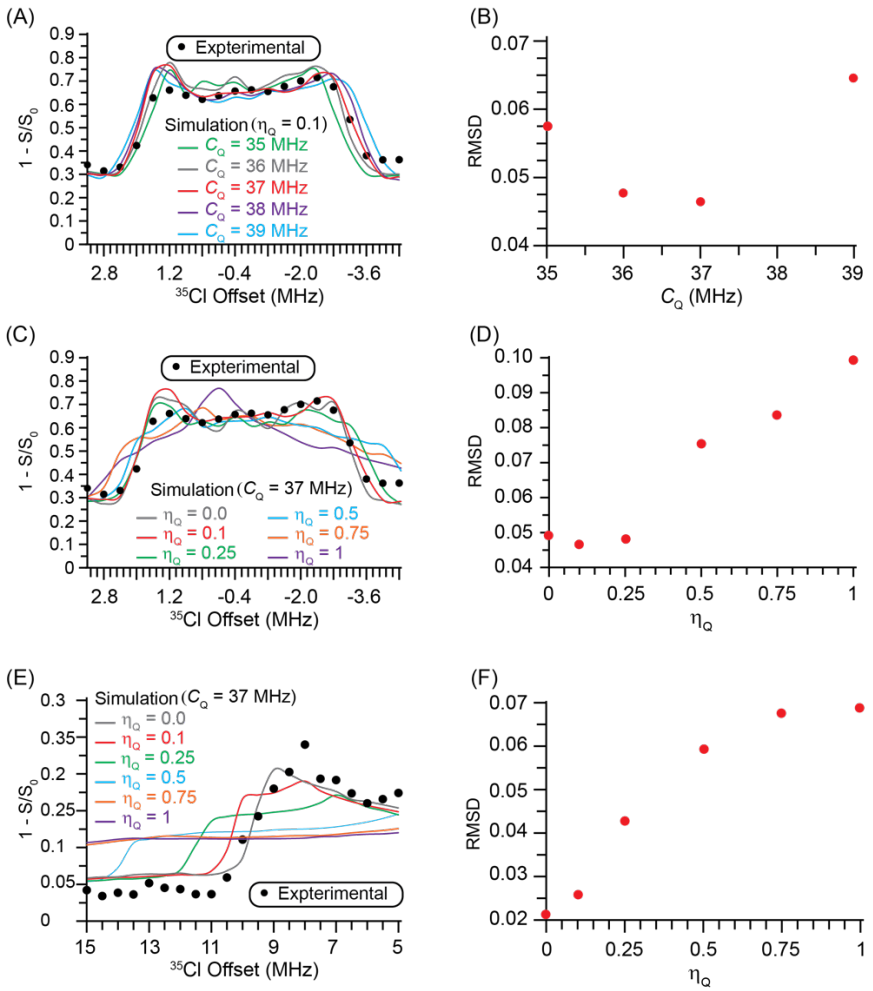

Figure S4. Simulations of ^{1}H{^{35}Cl} DE-RESPDOR dephasing profiles of transplatin (from Figure 3 of the main text) with different C_Q and η_Q values. (A) Plot of ^{1}H{^{35}Cl} DE-RESPDOR signal dephasing. The circles (black) and lines correspond to experimental data points and numerical simulation for a ^{35}Cl η_Q of 0.1 with C_Q values of 35 MHz (green), 36 MHz (grey), 37 MHz (red), 38 MHz (purple), 39 MHz (cyan). (B) The plot of root mean square deviation (RMSD) of the simulations as a function of the ^{35}Cl C_Q. (C) The circles (black) and lines correspond to experimental data points and numerical simulation for a ^{35}Cl C_Q of 37 MHz with η_Q values of 0.0 (grey), 0.1 (red), 0.25 (green), 0.5 (cyan), 0.75 (gold), 1.0 (purple). (D) Plot of RMSD for η_Q values of 0.0, 0.1, 0.25, 0.5, 0.75, and 1.0 with a fixed ^{35}Cl C_Q of 37 MHz. (E) ^{1}H{^{35}Cl} DE-RESPDOR dephasing profile for the ST region. The circles (black) correspond to experimental data points and lines correspond to numerical simulation for a ^{35}Cl C_Q of 37 MHz with η_Q = 0.0 (grey), 0.1 (red), 0.25 (green), 0.5 (cyan), 0.75 (gold), 1.0 (purple). (F) Plot of RMSD as for η_Q values of 0.0, 0.1, 0.25, 0.5, 0.75, and 1.0, with a fixed ^{35}Cl C_Q of 37 MHz.

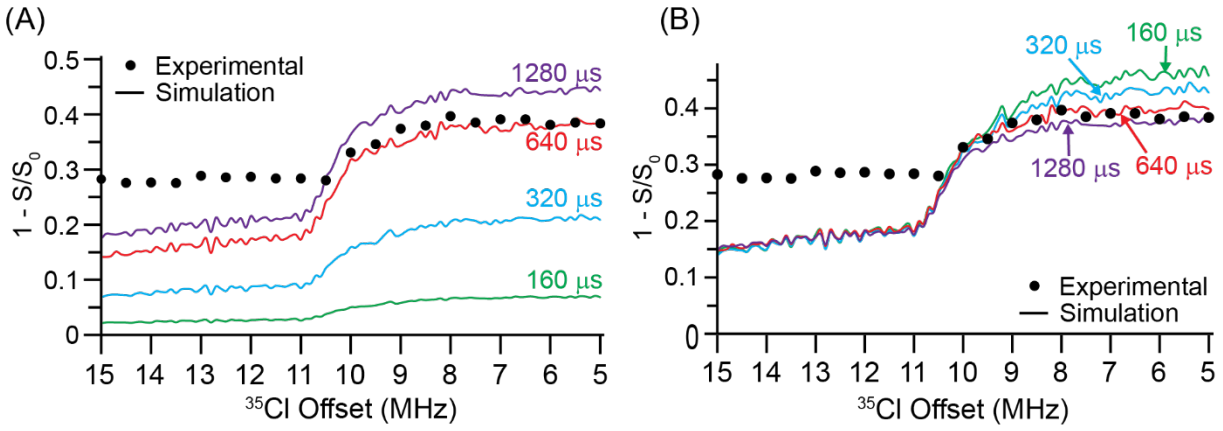

Figure S5. (A, B) Plot of experimental and simulated ^{1}H{^{35}Cl} DE-RESPDOR signal dephasing as a function of the ^{35}Cl transmitter recorded at B_0 = 9.4 T with 50 kHz MAS frequency for transplatin. The black circles correspond to experimental data points. The lines correspond to numerical SIMPSON simulation with total $SR4_1^2$ recoupling durations of 160 μs (green), 320 μs (cyan), 640 μs (red), and 1280 μs (purple). The simulations used a ^{1}H-^{35}Cl spin system with a 2 kHz dipolar coupling constant, C_Q = 37 MHz and η_Q = 0.1. In (A), we show unscaled dephasing, while in (B) the dephasing was scaled so that the dephasing at offsets between 11 MHz and 15 MHz was approximately constant. The different recoupling durations result in different extents of dephasing at the offsets from 5 MHz to 10 MHz. However, the position of the vertical discontinuity is approximately the same in all cases.

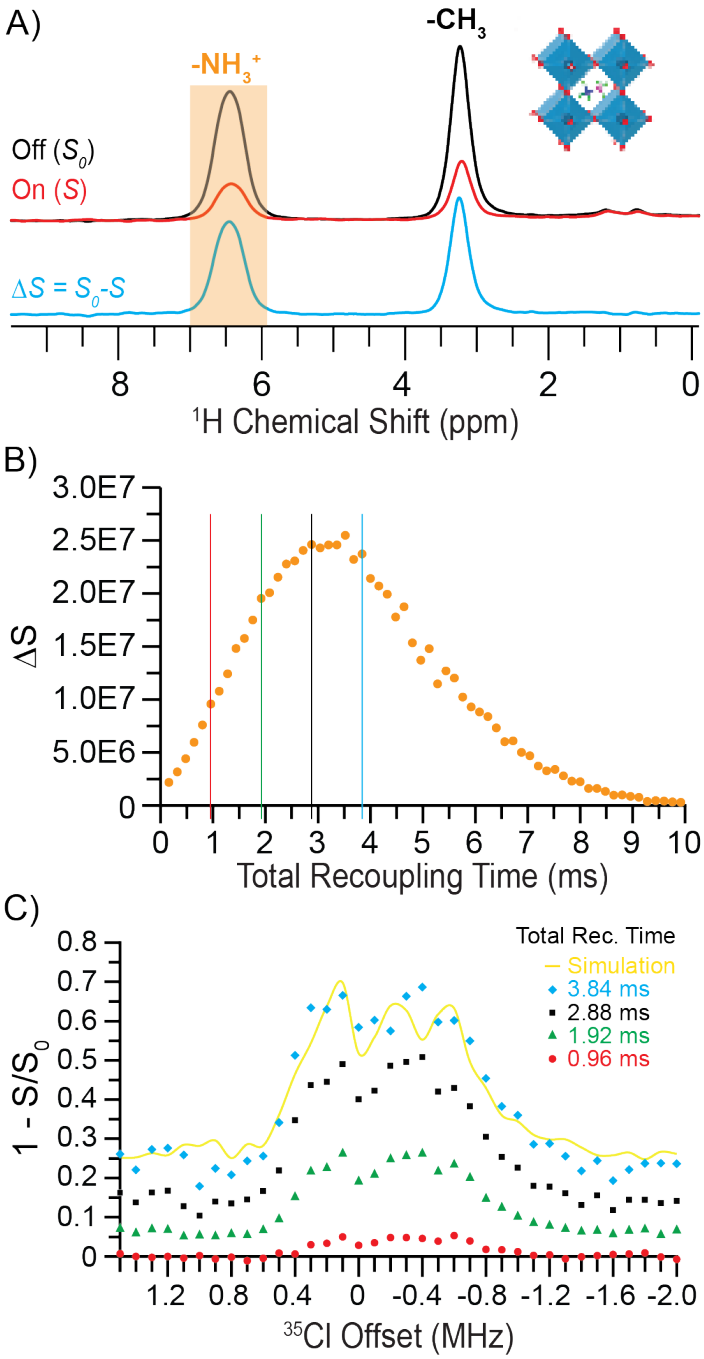

Figure S6. (A) 1D ^{1}H{^{35}Cl} DE-RESPDOR NMR spectra recorded (red) with or (black) without a ^{35}Cl saturation pulse and 2.4 ms of $SR4_1^2$ dipolar recoupling for $MAPbCl_3$. The ^{35}Cl saturation pulses were 80 μs in duration with a RF field of 80 kHz. A difference spectrum (cyan) is shown below. (B) Absolute dephasing (ΔS) as a function of total recoupling time in steps of 0.16 ms out to a total of 9.92 ms. (C) The plots of ^{1}H{^{35}Cl} DE-RESPDOR signal dephasing as a function of the ^{35}Cl offset recorded at B_0 = 9.4 T with 50 kHz MAS frequency. The circles (red), triangles (green), squares (black), and diamonds (cyan) correspond to different dephasing experiments with 0.96, 1.92, 2.88, and 3.84 ms recoupling times, respectively. The yellow line corresponds to the numerical simulation for a ^{35}Cl C_Q of 16.5 MHz.

Figure S6-A shows $^{1}H\{^{35}Cl\}$ DE-RESPDOR spectra (red), with saturation pulses and spectra (black), without saturation pulses. The difference spectrum (cyan) shown below has a signal-to-noise ratio of 73, allowing for the indirect detection of ^{35}Cl in $MAPbCl_3$. The spectra shown in Figure S6-A correspond to the 0 MHz ^{35}Cl offset. All spectra were collected at B_0 = 9.4 T using a ^{35}Cl saturation pulse length of four rotor cycles (80 s) with an 80 kHz RF field and 3.84 ms of $SR4_1^2$ dipolar recoupling. The highlighted (orange) peak corresponding to ammonium was used to plot the graphs shown in Figure S6-B, and C. Figure S6-B shows absolute dephasing ($\Delta S = S_0 - S$) as a function of total recoupling time. We performed four DE-RESPDOR experiments with 0.96 (red), 1.92 (green), 2.88 (black), and 3.84 ms (cyan) different recoupling times to figure out the optimal duration for this system as illustrated in Figure S6(C). The highest dephasing out of these four experiments resulted when the total recoupling time was 3.84 ms. The numerical simulation (yellow) of the $^{1}H\{^{35}Cl\}$ DE-RESPDOR dephasing profile with finer ^{35}Cl transmitter offsets of 1 kHz indicates that the ^{35}Cl C_Q is *ca.* 16.5 MHz (with $\eta_Q = 0$).

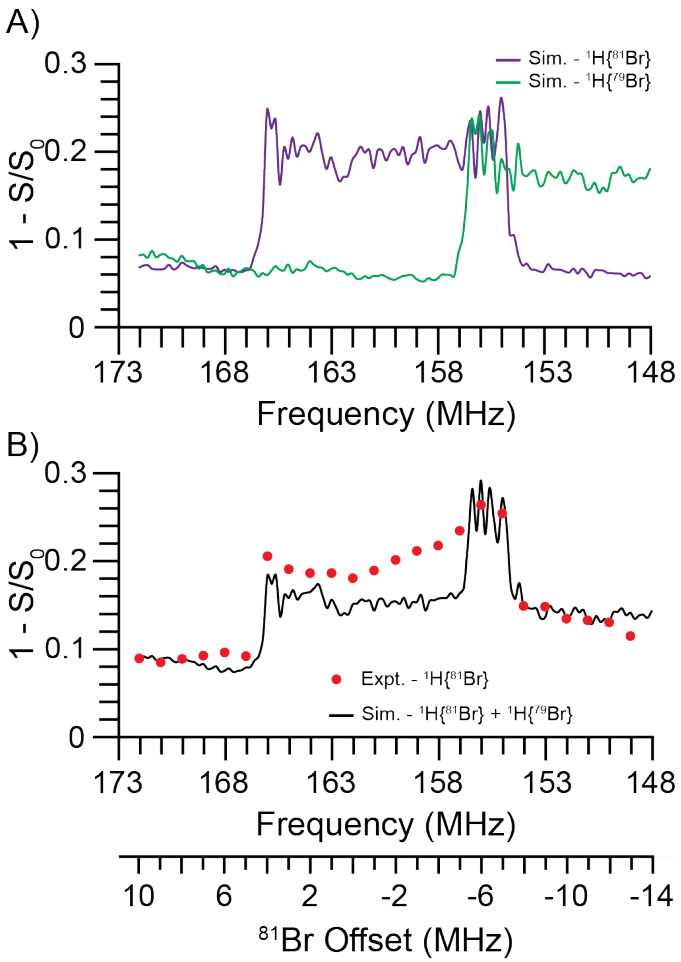

Figure S7. (A) Numerical simulation (purple) for a ^{81}Br C_Q of 118 MHz and the simulation (green) for ^{79}Br C_Q of 118 MHz (B) The plot of $^{1}H\{^{81}Br\}$ DE-RESPDOR signal dephasing as a function of the ^{81}Br transmitter recorded at B_0 = 14.1 T with 25 kHz MAS frequency. The circles correspond to experimental data points (red) and numerical simulation (black) for the sum of the $^{1}H\{^{81}Br\}$ and $^{1}H\{^{79}Br\}$ DE-RESPDOR dephasing.

Figure S7-B shows the experimental data points (red) and the numerical simulation (black) for the $^{1}H\{^{81}Br\}$ DE-RESPDOR experiment. Higher dephasing in the baseline can be seen due to the simultaneous excitation of the ^{79}Br and ^{81}Br at lower frequencies as demonstrated with the simulations in Figure. S7-A and B.

Synthesis and Single Crystal X-ray Structure of triphosCuI (1)

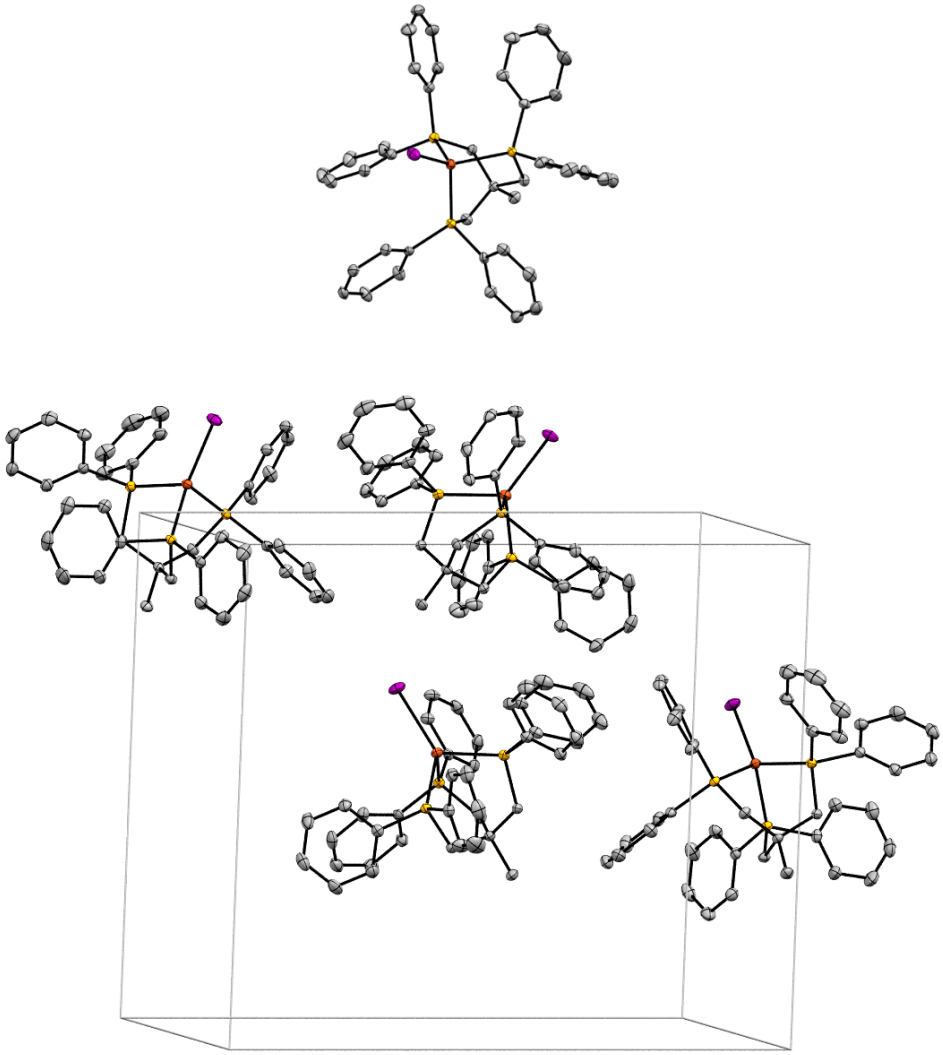

Figure S8. One molecule (top) and unit cell (bottom) of the single crystal X-ray structure of triphosCuI (**1**) [S5].

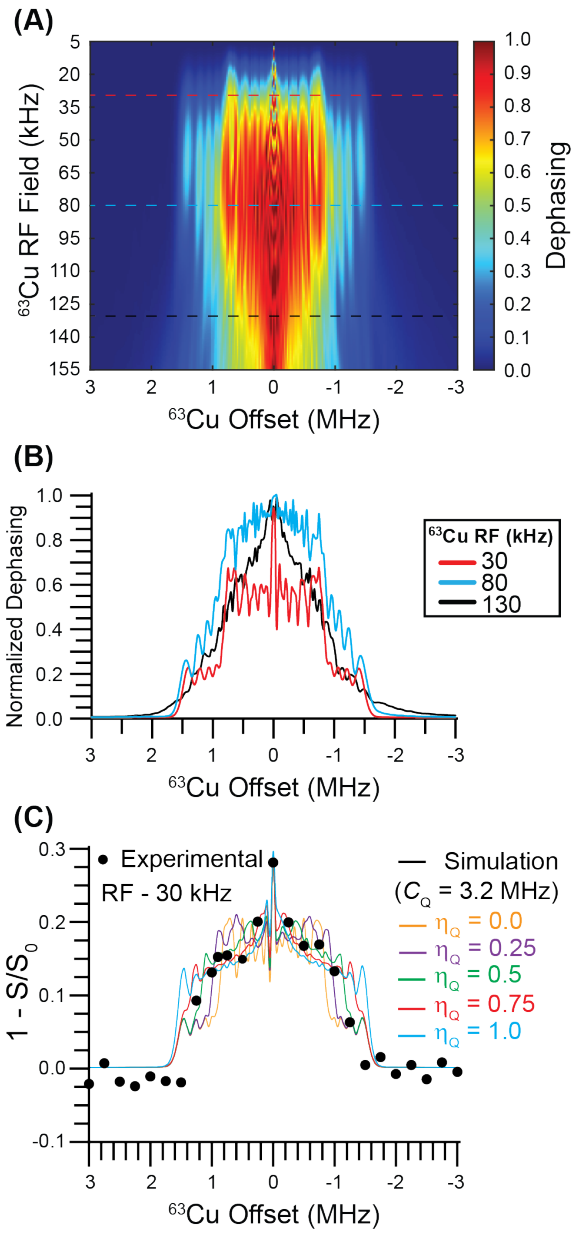

Figure S9. (A) Heat plots showing the SIMPSON simulated dephasing for ^{1}H→^{31}P{^{63}Cu} *J*-resolved experiments as a function of the ^{63}Cu saturation pulse RF field. Simulations are shown for conventional rectangular pulses 80 μs in duration. (B) Dephasing profiles extracted from the heat plots for ^{63}Cu saturation pulse RF fields 30 kHz, 80 kHz, and 130 kHz with rectangular saturation pulses. (C) The plot of ^{1}H→^{31}P{^{63}Cu} *J*-resolved signal dephasing as a function of the ^{63}Cu transmitter recorded at B_0 = 9.4 T with 25 kHz MAS frequency. The circles (black) and lines correspond to experimental data points and numerical simulation for a ^{63}Cu C_Q of 3.2 MHz with η_Q = 0.0 (gold), 0.25 (purple), 0.5 (green), 0.75 (red), 1.0 (cyan).

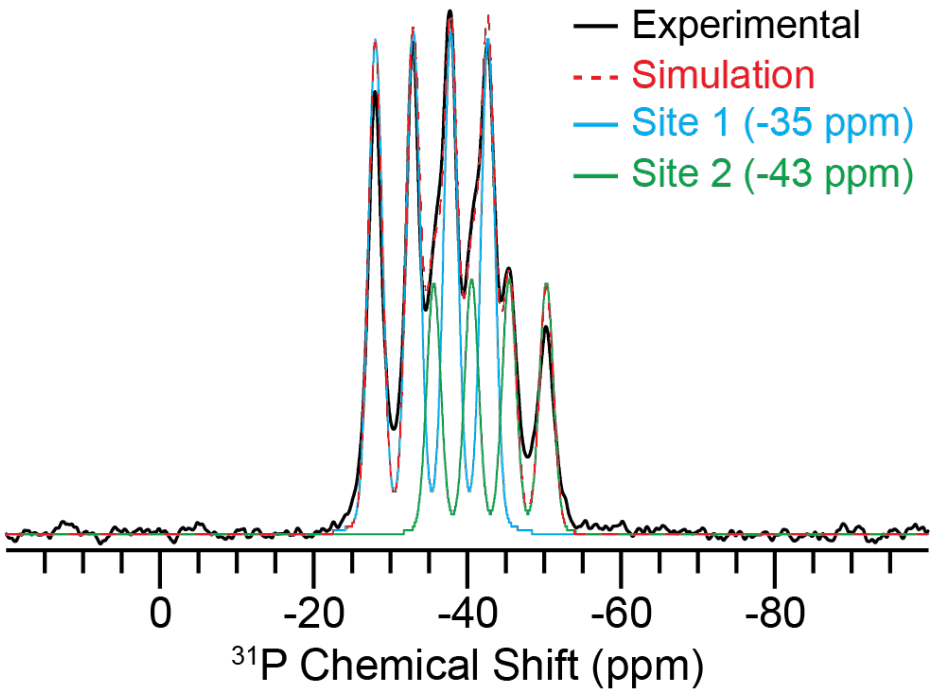

Figure S10. Experimental ^{31}P solid-state NMR spectrum (black) and simulated spectrum (red). The simulation was performed with the WSolids software package [S6]. The parameters used in the simulation are given in Table S2.

Table S2. Parameters for Simulation of the ^{31}P NMR Spectrum Shown in Figure S10.

^{31}P Chemical Shift (ppm)	–35		–43	
Relative Intensity (%)[a]	46.1	20.6	23.0	10.3
Coupled Nucleus	^{63}Cu	^{65}Cu	^{63}Cu	^{65}Cu
C_Q (MHz)	3.2	3.0	3.2	3.0
η_Q	0.57	0.57	0.57	0.57
Dipolar coupling (Hz)[b,c]	1092	1168	1092	1168
J-coupling (Hz)	800	855	800	855
ΔJ[c]	5	5	5	5

[a]For each ^{31}P chemical shift the intensity ratio of peaks coupled to ^{63}Cu and ^{65}Cu spins was fixed at the ratio of 2.244:1.00 to account for the natural isotopic abundance of the two Cu isotopes. The ^{31}P peak at –35 ppm was assumed to represent signals from two P atoms, while the signal at –43 ppm represented one P atom. Relative intensities were adjusted accordingly. [b]Dipolar coupling constants were calculated from the average P-Cu distance of 2.28 Å observed in the single-crystal X-ray diffraction structure. [c]Due to the relatively small magnitude of C_Q, the simulations are not sensitive to ΔJ or the values of the Euler angles (α and β) that relate the orientation of the dipolar coupling vector to the EFG tensor. Hence, α and β were assumed to be 0° and ΔJ was fixed at 5 Hz.

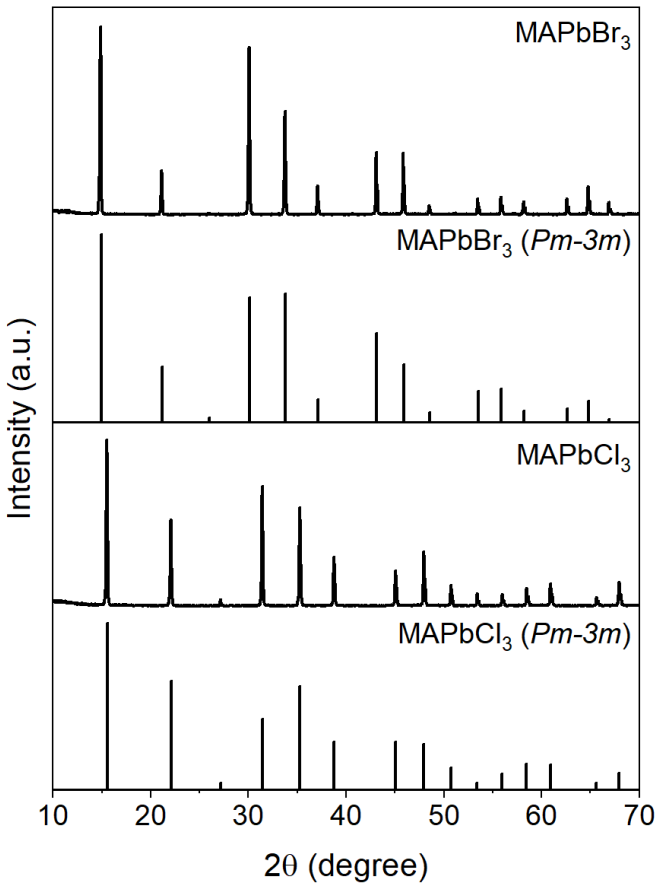

Figure S11. Experimental powder XRD patterns of $MAPbBr_3$ and $MAPbCl_3$ and standard *Pm-3m* $MAPbBr_3$ (ICSD #268785) and *Pm-3m* $MAPbCl_3$ (COD #7231905) for comparison.

Table S3. Comparison of acquisition times between DE-RESPROR and WURST-CPMG experiments

Figure	NMR Experiment	B_0(T)	MAS (kHz)	Inter-scan delay, $\tau_{rec.\ delay}$ (s)	# of scans	# of freq. steps/ retunes	Total Experiment Time (h)
Figure 3B	$^{1}H\{^{35}Cl\}$ DE-RESPDOR	9.4	50	5	8	20	0.4
Figure 3C	^{35}Cl WURST-CPMG	9.4	-	0.5	1024	21	3
Figure 4C	$^{1}H\{^{35}Cl\}$ DE-RESPDOR	9.4	50	5	8	36	0.4
Figure 4A	^{35}Cl WURST-CPMG	9.4	-	0.15	4096	5	0.9
Figure 4E	$^{207}Pb\{^{35}Cl\}$ *J*-resolved	9.4	25	2	2048	19	22.8
Figure 5A	^{81}Br WURST-CPMG	9.4	-	0.12	10240	2*	0.7
Figure 5C	$^{1}H\{^{81}Br\}$ DE-RESPDOR	14.1	25	10	8	24	1.1
Figure 6A	^{63}Cu DEPTH	9.4	25	3	4096	-	3.4
Figure 6C	$^{1}H\rightarrow^{31}P\{^{63}Cu\}$ J-resolved	9.4	25	10.4	16	26	1.2

*^{81}Br WURST-CPMG NMR spectra were only acquired at the position of the discontinuities of the central transition powder pattern.

Table S4. Experimental Solid-State NMR Parameters.

Figure	NMR Experiment	B_0(T)	MAS (kHz)	$\tau_{rec.\ delay}$ (s)	# of scans	# of freq. steps/ retunes	X sat. pulse (μs)	X RF Field (kHz)	Dipolar recoupling/ *J*-evolution time (ms)	Expt. Time (h)
Figure 3B	^{1}H{^{35}Cl} DE-RESPDOR	9.4	50	5	8	20	80	80	3.84	0.44
Figure 3C	^{35}Cl WURST-CPMG	9.4	-	0.5	1024	21	-	80	-	3
Figure 3D	^{1}H{^{35}Cl} DE-RESPDOR	9.4	50	5	8	21	80	80	3.84	0.47
Figure 3E	^{1}H{^{35}Cl} DE-RESPDOR	9.4	50	5	8	21	80[b]	80	3.84	0.47
Figure 4C	^{1}H{^{35}Cl} DE-RESPDOR	9.4	50	5	8	36	80	80	2.4	0.4
Figure 4A	^{35}Cl WURST-CPMG	9.4	-	0.15	4096	5	-	80	-	0.9
Figure 4E	^{207}Pb{^{35}Cl} *J*-resolved	9.4	25	2	2048	19	14	14	0.64[c]	22.8
Figure 5A	^{81}Br WURST-CPMG	9.4	-	0.12	10240	2[a]	-	50	-	0.7
Figure 5C	^{1}H{^{81}Br} DE-RESPDOR	14.1	25	10	8	24	50	50	1.92	1.1
Figure 6A	^{63}Cu DEPTH	9.4	25	3	4096	-	-	30	-	3.4
Figure 6C	^{1}H→^{31}P{^{63}Cu} J-resolved	9.4	25	10.4	16	26	30	30	1.44[c]	1.2

[a] ^{81}Br WURST-CPMG NMR spectra were only acquired at the position of the discontinuities of the central transition powder pattern.
[b] tanh/tan saturation pulses employed in this experiment.
[c] *J*-evolution time

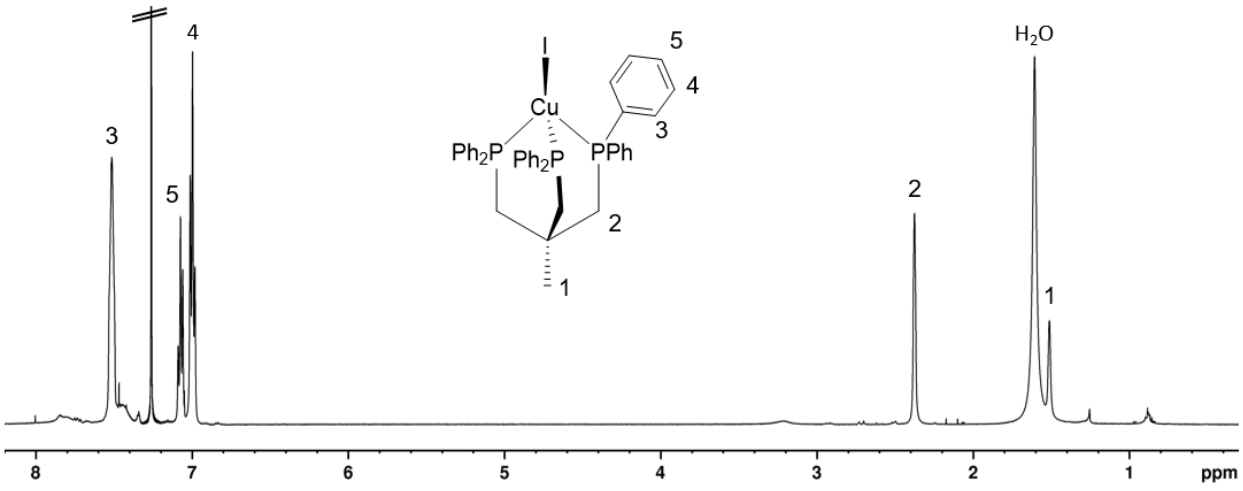

Figure S12. ^{1}H solution NMR spectrum of triphosCuI (**1**) in $CDCl_3$.

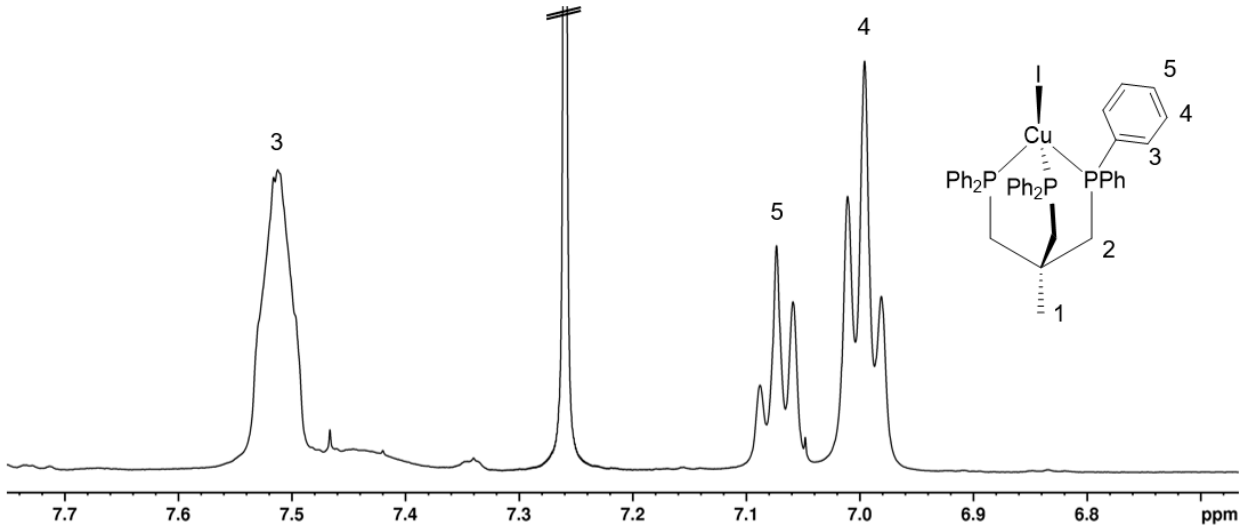

Figure S13. Expansion of the aryl region of the solution ^{1}H NMR spectrum of triphosCuI (**1**) in $CDCl_3$.

Solution NMR Spectroscopy. The ^{1}H solution NMR spectrum was recorded at 499.69 MHz on a 500 MHz Varian spectrometer at ambient temperature. Chemical shifts were referenced to the residual proton signal of the solvent ($CDCl_3$: $\delta(^{1}H)$ = 7.26 ppm).

Synthesis of triphosCuI (1)

A flask was charged with 1,1,1-tris(diphenylphosphinomethyl)ethane (111.3 mg, 0.1782 mmol), CuI (32.5 mg, 0.171 mmol), and 25 mL of chloroform under nitrogen. The reaction mixture was stirred overnight, forming a crystalline precipitate. The mixture was filtered, and the solids were washed with 3 mL of chloroform, then dried *in vacuo*. A colorless powder (103.5 mg, 0.1270 mmol, 71.3%) was collected.

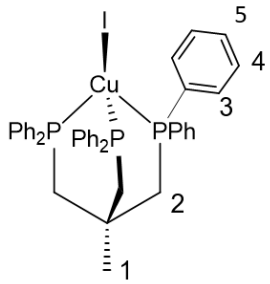

NMR (δ, $CDCl_3$), ^{1}H 7.51 (m, 12H, H3), 7.07 (t, 6H, H5, ^3J(H5-H4) = 7.3 Hz), 7.00 (t, 12H, H4, ^3J(H4-H5) = ^3J(H4-H3) = 7.3 Hz), 2.37 (s, 6H, H2), 1.51 (s, 3H, H1). Poor solubility and rapid exchange in solution prevented measurement of heteronuclei in solution.

X-Ray Crystallography [S5]

1. Crystals suitable for X-ray diffraction were obtained by slow evaporation from a chloroform solution. A Leica M80 microscope was used to identify a suitable single colorless block-shaped crystal of **1** showing well-defined faces with the dimensions $0.05 \times 0.04 \times 0.03$ mm^3 from a representative sample of crystals of the same habit. The crystal mounted on a nylon loop was then placed in a cold nitrogen stream (Oxford) maintained at T = 110.00 K.

Crystal screening, unit cell determination, and data collection were carried out using a Bruker Venture (PHOTON III) diffractometer. The diffraction pattern was indexed and the total number of runs and images was based on strategy calculation from the program APEX 3 [S1].

Data were measured using *f* and *w* scans with CuK_a radiation. Data was collected to a maximum resolution of $Q = 70.084^{\circ}$ (0.82 Å). The unit cell was refined using SAINT V8.38A on 9207 reflections, 147% of the observed reflections [S2].

Integrated Intensity information for each reflection was obtained by reduction of data frames using SAINT V8.38A [S2]. The final completeness is 99.90% out to 70.084° in *Q*. A multi-scan absorption correction was performed using TWINABS-2012/1 [S3]. For component 1: wR_2(int) was 0.0577 before and 0.0362 after correction. For component 2: wR_2(int) was 0.1430 before and 0.0503 after correction. The Ratio of minimum to maximum transmission is 0.71. Final HKLF 4 output contains 41280 reflections, $R_{int} = 0.0515$ (29025 with I > 3sig(I), $R_{int} = 0.0487$). The absorption coefficient *m* of this material is 9.081 mm^{-1} at this wavelength (*l* = 1.54178Å) and the minimum and maximum transmissions are 0.539 and 0.753.

Systematic reflection conditions and statistical tests of the data suggested the space group $Pna2_1$ (# 33) that was confirmed by an XT structure solution program using dual methods [S4]. The structure was refined by full matrix least squares minimization on F^2 using version 2018/3 of XL [S4]. All non-hydrogen atoms were refined anisotropically. Hydrogen atom positions were calculated geometrically and refined using the riding model.

Several crystals were tried and all of them showed non-merohedral twinning. Data was collected on a twinned crystal. Both the twin domains were used for data integration. TWINABS (as implemented in APEX 3) was used for absorption correction and to generate a hklf4 file with only non-overlapping reflections, and a hklf5 file with all the reflections from the major component. While the former was used for structure solution, the latter was used for the final least-squares refinement.

TWINABS-2012/1 was used for absorption correction [S3]. For component 1: wR_2(int) was

0.0577 before and 0.0362 after correction. For component 2: wR_2(int) was 0.1430 before and 0.0503 after correction. The Ratio of minimum to maximum transmission is 0.71. The final HKLF 4 output contains 41280 reflections, with R_{int} = 0.0515 (29025 with I > 3sig(I), R_{int} = 0.0487).

Table S5. Crystallographic data for **1** [S5].

	1
Deposition #	CCDC 2250183
empirical formula	$C_{41}H_{39}CuIP_3$
formula weight [g]	815.07
temperature [K]	110.0
diffractometer	Bruker Venture
wavelength [Å]	1.54178
crystal system	Orthorhombic
space group	*Pna2₁*
unit cell dimensions:	
a [Å]	20.3125(9)
b [Å]	10.3043(5)
c [Å]	17.1562(8)
α [°]	90
β [°]	90
γ [°]	90
V [Å^3]	3590.9(3)
Z	4
Z'	1
ρ_{calc} [Mg/m^3]	1.508
μ [mm^{-1}]	9.081
crystal size [mm^3]	0.05 × 0.04 × 0.03
Θ limit [°]	4.353 to 70.084
reflections collected	6246
independent reflections	6246
R(int)	0.0515
completeness to Θ	99.90 %
max. and min. transmission	0.539 and 0.753
data/restraints/parameters	6246 / 1 / 417
goodness-of-fit on F^2	1.036
R indices (final) [$I > 2\sigma(I)$]	
R_1	0.0223
wR_2	0.0566
R indices (all data)	
R_1	0.0237
wR_2	0.0573
largest diff. peak and hole [eÅ^{-3}]	0.461 and –0.242

Supporting Information References

[S1] Bruker (2018), *APEX3*, Bruker AXS Inc., Madison, Wisconsin, USA.

[S2] Bruker (2018), *SAINT*, Bruker AXS Inc., Madison, WI, USA

[S3] Bruker (2012), *TWINABS*, Bruker AXS Inc., Madison, WI, USA.

[S4] Sheldrick, G.M., ShelXL*, Acta Cryst.*, (2015), **C71**, 3-8. G. M. Sheldrick (2015), ShelXT, *Acta Cryst.* A**71**, 3-8. BRUKER AXS Inc., 5465 East Cheryl Parkway, Madison, WI 53711-5373 USA.

[S5] The CCDC reference number 2250183 contains the supplementary crystallographic data for the copper complex $CH_3C(CH_2PPh_2)_3CuI$ (triphosCuI) for this paper. This data can be obtained free of charge from the Cambridge Crystallographic Data Centre via www.ccdc.cam.ac.uk/data_request/cif.

[S6] WSolids1 ver. 1.21.7, K. Eichele, Universität Tübingen, 2021